[CANCER RESEARCH 61, 4190–4196, May 15, 2001]

Identification and Validation of *P311* as a Glioblastoma Invasion Gene Using Laser Capture Microdissection[1]

Luigi Mariani, Wendy S. McDonough, Dominique B. Hoelzinger, Christian Beaudry, Elzbieta Kaczmarek, Stephen W. Coons, Alf Giese, Mojdeh Moghaddam, Rolf W. Seiler, and Michael E. Berens[2]

Neurooncology Laboratory [L. M., W. S. M., D. B. H., C. B., E. K., M. E. B.], Department of Neuropathology [S. W. C.], Barrow Neurological Institute, Phoenix, Arizona 85013; Neurochirurgische Klinik, Universitäts-Krankenhaus Eppendorf, 20246 Hamburg, Germany [A. G.]; National Human Genome Research Institute, NIH, Bethesda, Maryland 20892 [M. M.]; and University Hospital, Inselspital, 3010 Bern, Switzerland [R. W. S.]

ABSTRACT

The mRNA expression profiles from glioblastoma cells residing at the tumor core and invasive rim of a human tumor resection were compared. From a single tumor specimen, 20,000 single cells from each region were collected by laser capture microdissection. Differential expression of 50–60 cDNA bands was detected. One of the sequences overexpressed by the invasive cells showed 99% homology to the *P311* gene, the protein product of which is reported to localize at focal adhesions. Relative overexpression of *P311* by invading glioblastoma cells compared with tumor core was confirmed by quantitative reverse transcription-PCR of six glioblastoma specimens after laser capture microdissection collection of rim and core cells. *In vitro* studies using antisense oligodeoxynucleotides and integrin activation confirmed the role of *P311* in supporting migration of malignant glioma cells. Immunochemistry studies confirmed the presence of the P311 protein in tumor cells, particularly at the invasive edge of human glioblastoma specimens.

INTRODUCTION

Failure in surgical cure of malignant gliomas is mainly due to those tumor cells that have invaded the normal brain far beyond the resectable areas (1–3). These remaining cells also resist radio- and chemotherapy and eventually lead to tumor regrowth and the patient's demise within <1 year from diagnosis (4–6). The identification of the mechanisms used by glioma cells to invade the brain could potentially indicate therapeutic strategies to reduce further spreading and/or to target the invading cells more specifically.

Investigations of tumor cell motility in general, and glioma invasion in particular, are mainly addressed using *in vitro* strategies. Such efforts led to the discovery and characterization of a significant number of molecules involved in glioma migration and potentially glioma invasion (7–12). However, *in vitro* strategies have some important limitations. One of these is the failure to reproduce the cerebral environment, which is likely to represent a unique determinant for the invading glioma cells.

To elucidate the mechanisms of glioma invasion *in vivo*, we coupled the capacity of LCM[3] to harvest single glioblastoma cells residing in the tumor core and at the invading edge with classical gene discovery techniques such as mRNA differential display and QRT-PCR (13). We were able to identify a number of known and unknown gene candidates potentially involved in glioma invasion. In this ongoing effort, we confirmed a role in glioma migration *in vitro* for one of these first gene candidates, the protein P311.

Received 8/22/00; accepted 3/19/01.

The costs of publication of this article were defrayed in part by the payment of page charges. This article must therefore be hereby marked *advertisement* in accordance with 18 U.S.C. Section 1734 solely to indicate this fact.

[1] A portion of this work represents the doctoral dissertation of E. K., University of Hamburg. L. M. is funded by a Grant of the Swiss National Research Foundation.

[2] To whom requests for reprints should be addressed, at Division of Neurology Research, Barrow Neurological Institute, 350 West Thomas Road, Phoenix, AZ 85013. Phone: (602) 406-6664; Fax: (602) 406-7172; E-mail: mberens@chw.edu.

[3] The abbreviations used are: LCM, laser capture microdissection; RT, reverse transcription; QRT-PCR, quantitative reverse transcription-PCR; ECM, extracellular matrix; ODN, oligodeoxynucleotide; FBS, fetal bovine serum; HGF/SF, hepatocyte growth factor/scatter factor.

MATERIALS AND METHODS

LCM

Cryopreserved glioblastoma specimens from seven patients were cut in serial 6–8-μm sections and mounted on uncoated slides treated with diethyl pyrocarbonate. The tumor core and adjacent invasive rim were identified on a coverslipped H&E-stained section (Fig. 1). One specimen was selected for collection of 20,000 individual cells for mRNA isolation and differential display analysis; the other specimens were used for quantitative, differential RT-PCR analysis. Cryostat sections intended for LCM were transferred from −80°C storage and immediately immersed in 75% ethanol at RT for 30 s. Slides were rinsed in H_2O, stained with filtered Meyer's hematoxylin for 30 s, rinsed in H_2O, stained with bluing reagent for 20–30 s, washed in 70 and 95% ethanol for 1 min each, stained with eosin Y for 20–30 s, dehydrated in 95% ethanol (twice for 1 min each), 100% ethanol (stored over molecular sieve; three times for 1 min each) and Xylene (three times for 10 min each). Slides were air dried under a laminar flow for 10–30 min and immediately processed for LCM. Diethyl pyrocarbonate-treated, autoclaved, distilled water was used to prepare every solution.

LCM was performed with a PixCell II Microscope (Arcturus Engineering, Inc., Mountain View, CA) using a 7.5-μm laser beam at 50–100 mV. Cells in the tumor core were readily identified and captured; tumor cells immediately adjacent to necrotic areas, cortical areas, or cells with a small regular nucleus, endothelial cells, and blood cells were avoided. Neoplastic astrocytes in the invasive rim ~1 cm from the edge of the tumor core were identified according to the criteria of nuclear atypia (coarse chromatin, nuclear pleomorphism, multinucleation) and, whenever possible, according to nuclear and/or cytoplasmic similarity with the glioblastoma cells in the core.

Differential Display of mRNA

Total RNA was isolated from the LCM-collected samples using StrataPrep (Stratagene) according to manufacturer's directions. Generation of cDNA segments and amplification of these pieces by PCR was done as previously described (14). Briefly, 100 ng of total RNA from each population were added to duplicate reactions, each containing the H-T_{11}A oligo(dT) primer anchored to the beginning of the poly(A) tail. RT-PCR was used to synthesize random primed segments of cDNA per manufacturer's directions (GeneHunter RNAimage, Nashville, TN). Each RT mix was aliquoted, combined with one of eight different AP primers, and tagged with [^{33}P]dATP. A display of the cDNAs was generated in the form of bands on a 6% polyacrylamide-urea gel (Fig. 2). Reproducible bands that were differentially expressed in either of the cell populations were excised from the gel, reamplified using the appropriate matching AP primer and H-T_{11}A primer from the RNA image kit, then cloned using a TA Cloning Kit (Invitrogen, San Diego, CA). Bacterial colonies were plated on agar containing 50 μg/ml ampicillin and 40 μl of 40 mg/ml 5-bromo-4-chloro-3-indolyl-β-D-galactopyranoside. Colonies carrying the plasmids with inserts (white) were harvested, expanded, verified using *Eco*RI restriction digestion, and sequenced using a CEQ2000 automated sequencer (Beckman). From these candidates, a band of interest, a 318-bp sequence with 99% homology (302 of 305 bp) to *P311* was elected for in-depth analysis.

QRT-PCR

Quantification. Real-time quantitative PCR was performed using the LightCycler (Roche) with fluorescence signal detection (SYBR green) after each cycle of amplification. Quantification was focused on the initial exponential phase of

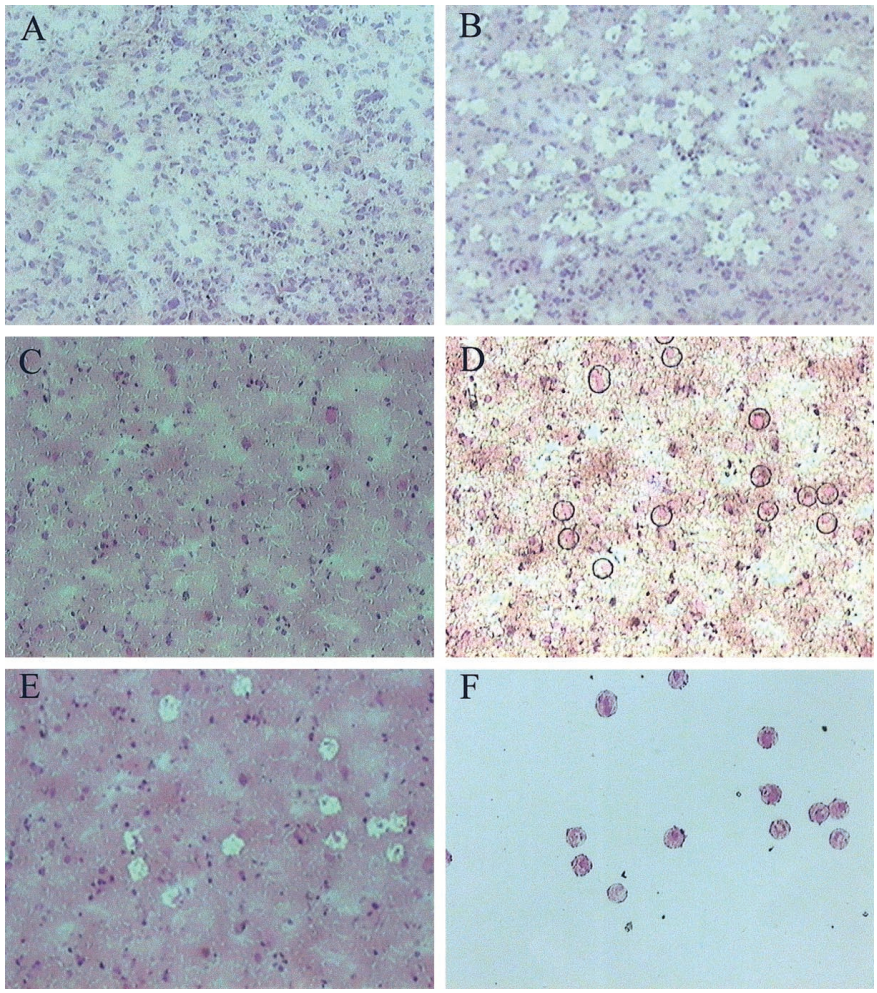

Fig. 1. Tumor core in specimen 15 before (*A*) and after (*B*) LCM. The invasive edge of the tumor is shown before microdissection in *C*, after laser-induced melting of the overlying polymer cap in *D*, and after lifting the polymer cap in *E*. *F*, captured cells. H&E staining of frozen sections 6 μm thick, $\times$20.

amplification above baseline according to the LightCycler software (15–17) and as described recently (13, 18). The calculated cDNA copy number in each sample was derived from an extrapolated crossing point of a mathematically derived line extending from the exponential phase of amplification in a plot of fluorescence intensity (SYBR green) *versus* cycle number. For each reaction, diluted amounts of known templates provided quantitative standard curve reactions and for each gene of interest from which cDNA copy number in clinical samples could be determined. Histone H3.3 was used as a housekeeping gene to normalize the initial content of total cDNA in the samples. The relative expression ratio between the invasive rim and the tumor core (rim:core ratio, *R*) was calculated as $R = X/Y$, where $X = P311$ copy number in the rim and $Y = P311$ copy number in the core, both normalized to equivalent amounts of histone H3.3.

PCR Conditions and Reagents. Total RNA was isolated from LCM-collected cells or cultured glioma cells using StratePrep. Primer sequences for *P311*: sense 5′-GACTGACTTCTTCGTTTCTT-3′, antisense 5′-CTTACAGCTTGCGTATTTATTGAACT-3′ (amplicon size, 278 bp). PCR conditions for *P311*: 95°C for 30 s, 70°C for 7 s, 72°C for 20 s, 40 cycles, followed by the melting curve analysis. Primers for histone H3.3: sense 5′-CCACTGAACTTCTGATTCGC-3′, antisense 5′-GCGTGCTAGCTGGATGTCTT-3′ (amplicon size, 215 bp). PCR conditions for histone H3.3: 95°C for 30 s, 64°C for 6 s, 72°C for 20 s, 40 cycles. Reference template standards for quantitative analysis of the genes of interest were prepared by cloning the *P311* and histone H3.3 cDNA sequences into pCR 2.1 TOPO TA vector (Invitrogen). After expansion in *Escherichia coli*, plasmids were extracted and linearized, and the concentration of DNA was determined by absorption at 260 nm. PCR was performed on 2 μl of cDNA in a final volume of 20 μl. Analysis of the melting curves (standards *versus* sample and negative control) ensured specificity of the amplification for the expected product (15). Additionally, agarose gel electrophoresis of the PCR products, followed by staining with ethidium bromide, was performed to confirm the specificity of the amplification.

Induction of Migration on Cell-derived ECM and Expression of *P311*

To create a coating of cell-derived ECM proteins, T25 culture flasks were seeded with SF767 glioma cells (19, 20). These were grown in MEM supplemented with 10% FBS to postconfluence and then removed by treatment with

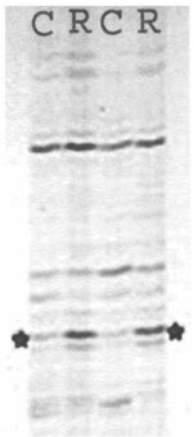

Fig. 2. Differential display analysis of mRNA. RNA-differential display analysis of LCM-collected cells from the tumor core (*C*) and invasive rim (*R*) of a human glioblastoma specimen. Isolated RNA from the LCM-collected material was equally divided, then processed in duplicate to determine reproducibility of the differential display. The cDNA band indicated between the two *stars* was excised and amplified using H-T_{11}A and AP2 primer sets. The cDNA sequence of this band appeared to be overexpressed by the invasive tumor cell population compared with the cell population of the tumor core. The sequence of this cDNA showed a 99% homology with the coding sequence of the *P311* gene.

0.5% Triton X-100 for 30 min at RT, followed by 0.25 M NH_4OH for 3–5 min at RT and thorough rinsing with PBS. The flasks covered with cell-derived ECM proteins stabilized with PBS were stored at 4°C until use. G112 glioma cells were seeded either on untreated T25 flasks or on ECM-coated T25 flasks to induce a migratory phenotype. The cells were grown to 30–50% confluence and then trypsinized and processed for RNA isolation and subsequent quantitative RT-PCR analysis for *P311* and histone H3.3 as described above.

Immunhistochemistry and Immunocytochemistry Studies

Fresh frozen tissue blocks were sectioned (6 μm thick) onto slides and then fixed in freshly prepared paraformaldehyde (2%) for 30 min and rinsed with PBS. Sections were incubated at RT in 0.1% Triton X-100 for 10 min, in 0.3% hydrogen peroxide in water, and then in 1% goat serum in PBS at room temperature for 30 min. After a rinse in PBS, slides were incubated in rabbit anti-P311 antisera overnight at 4°C [lot 1931 generated against the COOH-terminal peptide CGSSELRSPRISYLHFF of P311; Dr. Vande Woude (21); diluted 1:4000 in 1% goat serum in PBS (for test group) or in prebleed sera from the same rabbit before immunization at the same dilution (for negative control)]. The secondary antibody (biotin-conjugated goat antirabbit IgG; Vector Laboratories) was applied at a 1:400 dilution in 1% goat serum in PBS, followed by VECTASTAIN Elite ABC reagent (Vector Laboratories) according to the manufacturer's recommendations. Sections were counterstained with Mayer's hematoxylin and coverslipped.

About 2000–3000 SF767 and T98G glioma cells were seeded through a cell sedimentation manifold (see "Antisense Treatment and Migration Assays") on 10-well slides coated with either 1% BSA or human laminin (10 μg/ml). After 24–48 h, the cells were fixed with 2% paraformaldehyde for 10 min and then processed for P311 staining or mouse antivinculin (1:400, Sigma Chemical Co.) as described above. Negative controls were stained with a 1:50 dilution of preimmunization rabbit sera. Finally, the cells were incubated for 30 min with 1:100 dilution of FITC-conjugated antirabbit antibody or rhodamine-conjugated antimouse antibody (both from Roche Molecular Biochemicals). Images were collected using a Zeiss Axioplan fluorescence microscope (Zeiss, New York, NY) with filter sets 9 and 14, respectively.

Antisense Treatment and Migration Assays

Phosporothioate ODNs were designed from the coding sequence of the *P311* mRNA as follows: antisense ODN 5′-AAATGGTTCTTGACTGACCC-3′ (bp 231–250 of the *P311* coding sequence); sense ODN 5′-GGGTCAGTCAAGAACCATTT-3′; mismatched ODN 5′-GTACCGAATCCTAAGGCTT-3′. SF767, U251 MG, and U118 MG glioma cell lines were grown to 30–40% confluence in T25 flasks in MEM supplemented with 10% FBS. Cells were treated either with liposomes only (Lipofectin reagent; Life Technologies, Inc.) (20 μg/ml) or with liposomes containing ODNs for 6–12 h in MEM (serum-free) in a standard incubator. The cells were then trypsinized, counted, and seeded for the migration assay. An aliquot of collected cells was used for RNA isolation and quantitative RT-PCR for *P311* and histone H3.3 (see above).

The microliter scale migration assay has been described previously in detail (7) and has been recently used to verify an increased motility phenotype of melanoma cell lines with a more invasive phenotype *in vivo* (22). Ten-well slides were coated with 1% BSA or 10 μg/ml laminin at 37°C for 30 min and washed with PBS. Approximately 2500 cells/well were seeded into a cell sedimentation manifold (CSM Inc., Phoenix, AZ) to establish compact, confluent monolayers 1 mm in diameter. Cells were allowed to migrate during 24–48 h in MEM supplemented with 10% FBS in the incubator. The migration rate was calculated as the radius increase of the entire cell population over time. Experiments were performed as five replicates. At the end of the migration interval, the slides were fixed in 2% paraformaldehyde or 70% ethanol and processed for HE-staining, live-dead staining, or P311 immunofluorescence.

Viability Assays

The Live/Dead Cytotoxicity Kit (Molecular Probes) was used to determine cell viability following the migration assay on the 10-well slides. The medium was removed, the cells were washed twice with PBS, and the Live/Dead solution was added to the wells for 45 min. This assay provides a two-color fluorescence using the dyes calcein AM (green fluorescence for living cells) and ethidium homodimer. Ethidium homodimer-1 penetrates into cells with damaged membranes and undergoes a 40-fold enhancement of red fluorescence upon binding of nucleic acids of dead cells. After removal of the staining solution, the percentage of living and dead cells was determined by epifluorescent microscopy.

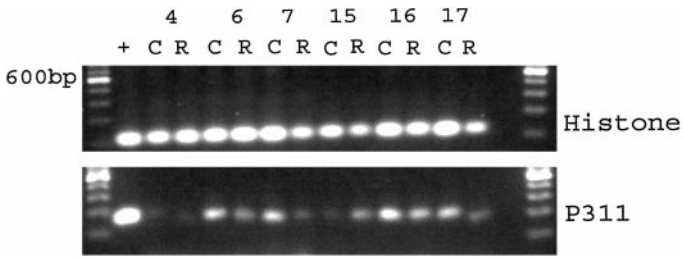

Fig. 3. Assessment of amplicon specificity after QRT-PCR. Agarose gel electrophoresis after staining with ethidium bromide is shown for each patient/specimen (*4*, *6*, *7*, *15*, *16*, and *17*). From 500 to 1000 glioblastoma cells were harvested from the tumor core (*C*) and the invasive rim (*R*) using LCM. Samples were processed for RNA isolation, followed by QRT-PCR for histone H3.3 (housekeeping gene for normalization) and *P311* (gene of interest). Melting curve analysis and agarose gel electrophoresis were used to verify amplicon purity and not to quantify the PCR product.

An Alamar blue assay (23) was used to assess cell viability of the SF767 glioma cells without treatment or after a exposure to either liposomes only (20 μg/ml) or *P311* antisense, sense, or mismatched ODNs. Briefly, cells were grown to 60% confluency before treatment with either liposomes only or in combination with 2.5 μM antisense, 2.5 μM sense, or 2.5 μM random oligonucleotides. After 4 h of treatment, 4000 cells of each population were seeded in quadruplicate wells of three 96-well flat-bottomed plates in 200 μl of culture medium supplemented with 10% FBS. The plates were incubated for 4, 20, and 32 h, respectively. Alamar blue was added in a volume of 20 μl (10% of total volume) to the cells at the various time points and incubated for 2 h. The plates were read on a fluorescence plate reader (excitation 530 nm; emission 590 nm). Averages of the fluorescent signals were calculated and plotted against a standard curve of untreated cells to assess live cell number.

Laser Scanning Cytometry

Laser scanning cytometry was used to quantitatively assess decreased levels of P311 protein during the migration assay after antisense treatment (Fig. 7*B*). After P311 immunofluorescent staining of the migration assays, the slides were analyzed using a laser scanning cytometer (CompuCyte, Cambridge, MA), which allows quantitative fluorescence signal processing of individual cells in a population on a flat surface. The laser scanner cytometer records the FITC fluorescence of each single cells on the well and counts the total number of cells on the well. The mean peak fluorescence of all of the cells in each well is calculated. The average of five wells was compared among untreated controls and the different treatments (Lipofectin only, antisense or mismatched ODNs) to determine changes in P311 protein levels.

Statistical Analysis

A two-tailed, unpaired *t* test compared the $\log_{10}$ value of ratios of gene expression. Differences between invasive rim and tumor core (*R*:*C* Ratio) were analyzed relative to the null hypothesis, which predicted a ratio of 1 ($\log_{10}$ ratio, 0).

RESULTS

Overexpression of *P311* by the Invasive Tumor Cells *in Vivo*. Discreet cDNA bands differentially expressed using the primer set H-T_{11}A and H-AP2 (clone R.2.1) were consistently identified in the rim cell population (Fig. 3). After elution, reamplification, and cloning, this cDNA fragment was sequenced. Homology of 99% (302 of 305 bp) was found between candidate R.2.1 and the coding sequence for *P311* (WWW Blast at National Center for Biotechnology Information; NM 004772). This protein has been described

in the context of embryonic neuronal migration (24) and of Met-HGF/SF signaling in SK-LMS cells (a leiomyosarcoma cell line) (21). *P311* is a 2036-bp mRNA encoding a 68-amino acid polypeptide with a very short half-life. Rapid turnover of *P311* is believed to be due to degradation by the proteasome-ubiquitin system and an unidentified metalloprotease (21).

Six glioma specimens were analyzed for relative levels of expression of *P311* in cells at the tumor core and invasive rim. The ratio of *P311* message template number (cDNA) in rim:core was almost invariably >1 in QRT-PCR analysis (Table 1); the mean *R*:*C* was 3.1 for the first round of analysis, RT1 (range ± SD 1.2–8.1) and 3.3 for the second round, RT2 (range ± SD 1.3–7.8). The $\log_{10}$ values of the ratios for each QRT-PCR were statistically different from the null hypothesis (*R*:*C*, 1) in the unpaired, two-tailed Student *t* test ($P = 0.018$ for RT1, $P = 0.016$ for RT2, $P = 0.0006$ for RT1 and RT2 combined).

To estimate the impact of a possible contamination of the "invasive rim" sample with normal brain cells, we compared the level of mRNA by QRT-PCR of samples from four normal brains (cortex and adjacent white matter retrieved within 2 h postmortem) and two glioblastomas. The level of *P311* mRNA in the normal brain averaged 1.83-fold higher than in the two glioblastomas (range ± SD 1.38–2.53; $P < 0.05$). The LCM-harvested tumor cells show an average 3.25-fold overexpression of *P311* in invasive cells compared with cells in the tumor core (range ± SD 1.3–8.1; $P = 0.0006$). Statistical comparison of these data sets indicates that the elevated expression of *P311* in the rim samples compared with tumor core is not due to contamination by normal brain in the rim ($P = 0.028$).

Furthermore, from the analysis of other genes of known overexpression in brain tumor cells compared with normal brain, the cells captured in the invasive rim are predominantly tumor cells in our samples (data now shown). The presence of *P311* mRNA in the adult brain has been described (24), but its role remains obscure.

Reduced Migration of Glioma Cell Lines Treated with Antisense *P311*-ODNs. Expression of *P311* in glioma cells is amenable to manipulation by treatment with antisense ODNs designed against the 3′ end of the *P311* mRNA. Human glioma cell line SF767 showed specific reduction in *P311* mRNA after treatment with antisense *P311* ODN compared with treatment with mismatched or sense ODNs (Fig. 4*A*). Human glioma cells treated with 2.5 μM ODNs only inhibited migration if the sequence was complimentary to *P311* (antisense; Fig. 4*B*). Migration inhibition occurred whether the cells were plated on a specific substrate (laminin) or a nonspecific substrate (coating with BSA). The magnitude of inhibition was dependent on the concentration of antisense *P311* ODNs (Fig. 5*A*). Quantitative immunofluorescence

Table 1 *Overexpression of P311 in invasive cells versus tumor core from human glioblastoma specimens*

Overexpression of the *P311* mRNA in invasive glioblastoma cells captured using LCM is expressed as a *R:C* ratio for six human specimens analyzed by quantitative RT-PCR in duplicate reactions (RT1 and RT2). The ratios are significantly higher than 1 in both RT reactions ($P = 0.018$ for RT1 and $P = 0.016$ for RT2; see "Materials and Methods" for statistical analysis).

	R:C ratio	
Specimen	RT1	RT2
4	3.14, 1.55[a]	1.95
6	3.52	1
7		1.9
15	19.4, 3.06[a]	9.7
16	3.2	7.4
17	0.85	4.7
Mean	3.1	3.3
Range (± SD)	1.2–8.1	1.3–7.8

[a] Repeat PCR run.

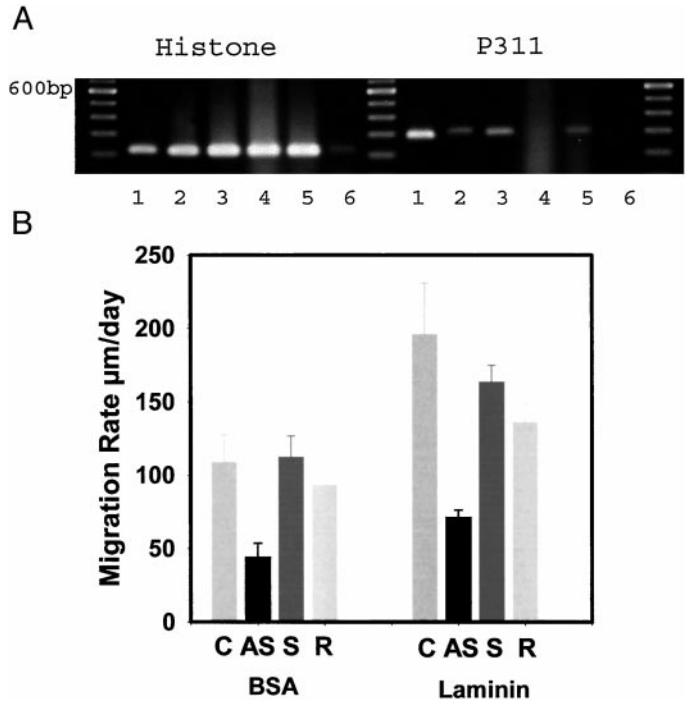

Fig. 4. Specific reduction of P311 mRNA and migration rate of SF767 cells with antisense treatment. *A*, agarose gel electrophoresis showing the PCR products for histone and *P311* in SF767 cells after either no treatment (*Lane 2*), treatment with liposomes 20 μg/ml (*Lane 3*), liposomes + antisense P311 ODNs (*Lane 4*), or mismatched ODNs at 2.5 μM (*Lane 5*). *Lanes 1* and *6*, positive (standards) and negative controls, respectively. Complete inhibition of P311 at the mRNA level is shown after antisense treatment only. *B*, migration rate of SF767 glioma cells on 1% BSA and 10 μg/ml laminin. The cells were treated (as above) with liposomes only (*C*, control) or in association with *P311*-antisense (*AS*), sense (*S*), or random (*R*) ODNs, respectively. The *P311*-antisense treatment resulted in a marked decrease of the migratory ability of SF767 cells compared with the controls (*t* test, unpaired, two-tailed, $P < 0.01$). *Bars*, 1 SD from the mean of five replicate migration assays. This experiment was repeated three times independently with similar results.

of P311 protein in SF767 glioma cells treated with antisense *P311* ODNs demonstrates loss of the P311 translation product (Fig. 5*B*). In a monolayer migration assay, a marked dose-dependent decrease in the migration rate of SF767 cells on laminin substrate was evident (Fig. 5*C*). The morphology of the anti-*P311* ODN-treated cells showed a marked decrease in the number of lamellopodia, resulting in a rounded or pilocytic rather than a polygonal shape compared with the controls (data not shown). The viability assays did not reveal any toxic effect due to the antisense *P311* ODNs compared with the random or sense ODN sequences (data not shown).

Overexpression of *P311* in Cells Activated to Migrate. Human glioma cell lines G112 and T98G were grown either in standard culture flasks or in flasks precoated with glioma-derived ECM. This coating enhances the motility behavior of these cells (25–27). Total RNA was isolated from these two cell populations for quantitative RT-PCR analysis of *P311* expression on replicate experiments. Culture of both glioma cell lines on motility-promoting substrate resulted in a significant overexpression of *P311* compared with the control in replicate experiments. For G112 cells, overexpression on ECM was 1.63-fold (range within 1 SD 1.05–2.52; $P = 0.015$) in one experiment, and 52-fold (range within 1 SD 28.9–93.6; $P = 0.02$) in a second. T98G cells on ECM overexpressed P311 mRNA by 7.5-fold (range within 1 SD 1.6–23.1; $P = 0.21$).

Immunochemical Localization of the P311 Protein in Frozen Sections of Glioblastoma Specimens and Glioma Cell Lines. Peroxidase-based immunohistochemistry studies on frozen sections of specimens 15 and 16 show a strong P311 staining confined to the

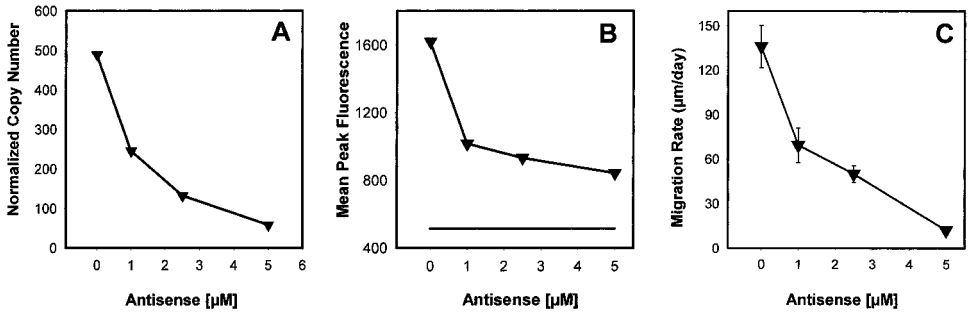

Fig. 5. Dose-dependent effects of P311 antisense ODN treatment on P311 mRNA and protein levels and migration rates of glioblastoma cells. In *A*, the number of *P311* mRNA copies (assessed by QRT-PCR) decreased after treatment with increasing doses of antisense P311 ODNs. In *B*, quantitative analysis by laser scanning cytometry of cells immunostained for *P311* also showed an inverse relationship between the level of P311 protein and the dose of antisense ODNs. Fluorescence intensities for each individual cell of the well containing a migration assay were recorded. The mean peak fluorescence of the cell population on the well was calculated. The average of five replicates (wells) is shown. The error bars within 1 SD are hidden by the triangular symbols. The controls (liposomes only and mismatched ODNs) did not show any reduction in P311 protein levels (not shown). In *C*, in parallel, the migration rate of SF767 glioma cells on laminin 10 μg/ml decreased in a dose-dependent manner after P311 antisense treatment compared with the controls. *Bars*, 1 SD from the mean of five replicates. This experiment was repeated twice with similar results.

cytoplasm of tumor cells in the core and at the invasive rim (Fig. 6). Individual cell staining is possibly stronger in tumor cells of the invasive rim; however, the potential intermingling of normal and reactive glial cells as well as neurons prevents unequivocal assessment of a quantitative labeling index for P311 at the invasive edge. P311 immunoreactivity was very low in the normal brain parenchyma (regions without obvious tumor infiltration).

Immunofluorescent staining of human glioma cell lines SF767 and T98G seeded on a migration-activating substrate of laminin, indicates a cytoplasmic localization of P311. Topographic projection of the confocal images illustrates that the nuclei of these cells are devoid of P311 immunoreactivity (data not shown). Simultaneous immunofluorescent staining of these cells for P311 and vinculin did not demonstrate definite colocalization at the focal adhesions (Fig. 7), a feature described by Taylor *et al.* (21) in normal human astrocytes in culture using the same reagents.

DISCUSSION

Improved understanding of the mechanisms used by glioma cells to invade the surrounding brain tissue is limited by the inability to reproduce this cerebral environment *in vitro*. In this study, we try to identify the genetic programs activated by glioma cells caught in the act of invading the brain tissue *in vivo*. We have used the capacity of LCM to harvest single cells from frozen sections coupled with differential display analysis of mRNAs isolated from the invading and noninvading tumor cells. A major potential impediment to successful use of LCM at the invasive edge of a glioblastoma specimen is due to the difficulty to reliably identify tumor cells, requiring their differentiation from normal/reactive astrocytes and other glial or neuronal cells on a frozen section (28, 29). This difficulty progressively increases the further away from the tumor edge into the normal parenchyma cell collection is

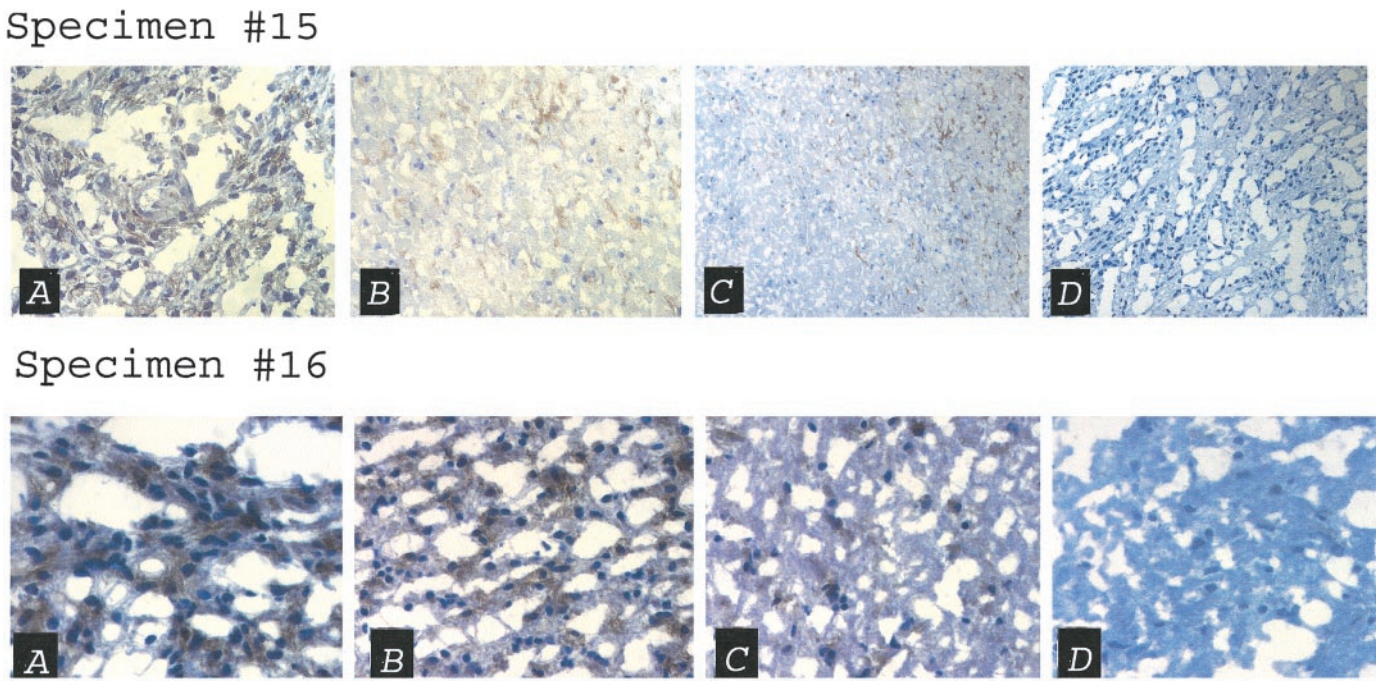

Fig. 6. Immunohistochemistry studies for P311 in glioblastoma specimens. Peroxidase-based immunostaining for P311 in frozen sections of specimens 15 and 16. *15A* and *15B*, tumor cells with positive, cytoplasmic P311 immunostaining in the tumor core and in the infiltration zone, respectively. ×40. The number of cells immunostained for P311 progressively diminishes whereas the distance from the tumor increases (*15C, left bottom corner*, ×20; *16C*, ×63). Although not quantitative, this pattern of staining suggests a higher level of P311 protein in tumor cells compared with glial cells with normal morphology. *D*, immunostaining with preimmune serum. *15D*, ×20; *16D*, ×63).

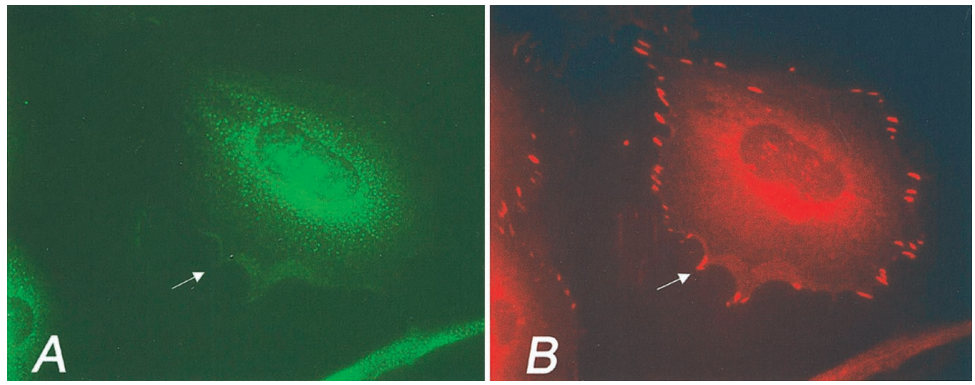

Fig. 7. *P311*-Immunofluorescence in glioma cells. T98G glioma cells migrating on a laminin substrate were stained using rabbit anti-P311 (*A*) and mouse antivinculin primary antibodies (*B*), followed by fluorescein-conjugated antirabbit and rhodamine-conjugated antimouse secondary antibodies, respectively. P311 immunofluorescence shows diffuse, punctate cytoplasmic staining in *A*. Colocalization of vinculin and P311 at the focal adhesions (*arrows*; a feature described by Taylor *et al.* in Ref. 21 in normal human astrocytes in culture) could not be demonstrated in T98G cells.

attempted. Retrieving single tumor cells from a frank glioblastoma by LCM is a straightforward procedure as opposed to capturing tumor cells from the invasive tumoral edge, which is time consuming and requires a sound interpretation of histopathology. The main potential caveat of this procedure is the risk of capturing normal brain cells. To reduce this risk, we captured cells in the immediate vicinity of the tumoral edge in the white matter. We selected cells with dysplastic nuclei and cells similar to those in the frank tumor tissue. The isolated RNA was of sufficient quality to perform differential display and quantitative RT-PCR for validation in additional human samples.

LCM of a cryopreserved glioblastoma specimen followed by mRNA differential display was successful in identifying gene candidates implicated in the invasion process. The differential display analysis showed that the vast majority of mRNAs (~800 fragments) were expressed at approximately the same level by the two cell populations. Against this background of homogeneity, 50–60 differentially expressed cDNA fragments were isolated, cloned, and sequenced. We initially selected a band corresponding to a fragment of the coding sequence of *P311* for in-depth investigation. Quantitative RT-PCR analysis of additional glioblastoma specimens confirmed overexpression of this gene in the invasive glioma cells harvested by LCM (Table 1).

The first of the three open reading frames of the *P311* cDNA is well conserved among different species (human, mouse, chicken) and encodes a 68-amino acid polypeptide. Such conservation argues for a fundamental function of the gene product.

P311 was first described by Studler *et al.* (24) as a transcript abundantly expressed by neuronal cells in the striatum and superficial cortical layers during gestational days 17–20. The authors concluded that this gene is overexpressed by neurons belonging to the late migration wave from the germinal to the cortical layers. They further described the persistence of this transcript in the cerebellar cortex, hippocampus, and olfactory bulb in the mouse. Because a high neuronal plasticity is known to occur in these locations, the authors hypothesized a role for P311 in this context. Taylor *et al.* (21) recently found that P311 is highly expressed by human intestinal smooth cells, normal human astrocytes in culture, and the leiomyosarcoma cell line SK-LMS. Expression of P311 was reduced in the SK-LMS cell line when cells were modified to have a high c-Met-HGF/SF signaling which can induce motility, invasiveness and angiogenesis (30–32). Neural precursor cells induced to terminally differentiate by NGF treatment also showed a reduction in P311 expression (21). However, single doses of HGF/SF did not result in a reduced mRNA expression of *P311* by the SK-LMS cell line.

Our finding of elevated P311 expression in invading glioblastoma cells relative to cells in the same tumor residing in the (noninvading) tumor core align with a putative role of this gene product in invasion, or possibly transient dedifferentiation to a more motile phenotype. The antisense ODN experiments argue that specific down-regulation of *P311* mRNA and protein levels suppresses migration. These findings accumulate to suggest that P311 expression may be elevated to achieve portions of the invasive cascade of these malignant cells. The immunohistochemical staining of the human glioblastoma specimens confirmed the presence of the P311 protein in the cytoplasm of tumor cells in the tumor core and particularly at the tumor edge. The rarity, and potentially the absence, of normal brain cells staining positively for P311 indicate that this protein is mainly produced by tumor cells and not by normal or reactive brain cells in the surrounding parenchyma. These findings argue for a null expression of P311 protein by normal astrocytes, although Taylor *et al.* (21) indicated that cultured astrocytes express *P311* message. Manipulation of human glioma cell migration behavior by culture on motility-enhancing substrates showed elevation in *P311* message. We speculate that P311 is a biochemical determinant of glial cell migration and/or invasion. Explanted normal astrocytes may manifest very active migratory behavior, which may explain the earlier report.

Mechanisms other than gene expression regulation may also impact the influence of P311 on glioma cell migration. These may include activation or suppression by phosphorylation, sequestration, or release of translated P311 gene product in response to signaling mediators in the cell, and reduced or increased degradation. A potential phosphorylation site at the COOH end of P311 indicates that this protein may be regulated by phosphorylation. The half-life of this protein appears to be very short due to proteasome and metalloprotease activity, below 5 min according to Taylor *et al.* (21).

Confocal microscopy studies indicated colocalization of the P311 protein with vinculin at the focal adhesion in normal human astrocytes in culture (21). Our studies demonstrate that when human glioma cells are cultured under migration-activated conditions, the localization of P311 is diffuse in the cytoplasm but not at the focal adhesions (Fig. 7). These findings suggest at least a putative role of P311 in glioma migration.

LCM allows capturing of circular areas surrounding nuclei without respecting cytoplasmic contours or cell membranes. Thus, we cannot exclude a possibility that the LCM-collected mRNA was actually sublocalized in the cytoplasmic periphery of normal brain cells as a response to the invading neoplastic cells. In this case, our findings would be suggestive of a reactive brain cell response to invading glioblastoma. The *in vitro* observations, however, refute this line of thinking because suppression of P311 expression retards glioma migration, and activation of migration up-regulates P311 expression in glioma cell lines.

Overall, our data suggest a specific role of P311 in activating glioma invasion through enhanced glioma cell motility. The absence of this protein in the focal adhesions (where it has been localized in

normal astrocytes in culture) along with its overexpression "*in vivo* " and "*in vitro* " during migration suggest a relocalization and possibly a switch in function. Further studies are needed to assess the role of this protein and its potential interactions with the cytoskeleton or soluble mediators of migration.

The success of the strategy used in this study opens new perspectives for research in the field of glioma invasion. We anticipate that more accurate identification of tumor cells with a highly invasive phenotype in tissue sections will be possible in the near future. This ability, coupled with modern techniques to assess differential gene expression using minuscule amounts of RNA, may lead to a better understanding of the mechanisms responsible for the unique invasive behavior of glioma cells *in vivo*.

Acknowledgements

We thank George F. Vande Woude and Gregory A. Taylor for providing us with the P311 antibodies and Jim Borree from CompuCyte for generating the laser scanner cytometry data.

REFERENCES

1. Silbergeld, D. L., and Chicoine, M. R. Isolation and characterization of human malignant glioma cells from histologically normal brain. J. Neurosurg., *86:* 525–531, 1997.
2. Berens, M. E., and Giese, A. ". . . those left behind." Biology and oncology of invasive glioma cells. Neoplasia, *1:* 208–219, 1999.
3. Gaspar, L. E., Fisher, B. J., MacDonald, D. R., LeBer, D. V., Halperin, E. C., Schold, S. C. J., and Cairncross, J. G. Supratentorial malignant glioma: patterns of recurrence and implications for external beam local treatment. Int. J. Radiat. Oncol. Biol. Phys., *24:* 55–57, 1992.
4. Glinski, B., Dymek, P., and Skolyszewski, J. Altered chemotherapy schedules in postoperative treatment of patients with malignant gliomas. Twenty-year experience of the Maria Sklodowska-Curie Memorial Center in Krakow. J. Neuro-oncol., *36:* 159–165, 1998.
5. Mornex, F., Nayel, H., and Taillandier, L. Radiation therapy for malignant astrocytomas in adults. Radiother. Oncol., *27:* 181–192, 1993.
6. Vick, N. A., and Paleologos, N. A. External beam radiotherapy: hard facts and painful realities. J. Neuro-oncol., *24:* 93–95, 1995.
7. Berens, M. E., Rief, M. D., Loo, M. A., and Giese, A. The role of extracellular matrix in human astrocytoma migration and proliferation studied in a microliter scale assay. Clin. Exp. Metastasis, *12:* 405–415, 1994.
8. Chicoine, M. R., and Silbergeld, D. L. The *in vitro* motility of human gliomas increases with increasing grade of malignancy. Cancer (Phila.), *75:* 2904–2909, 1995.
9. Friedlander, D. R., Zagzag, D., Shiff, B., Cohen, H., Allen, J. C., Kelly, P. J., and Grumet, M. Migration of brain tumor cells on extracellular matrix proteins *in vitro* correlates with tumor type and grade and involves α-v and β-1 integrins. Cancer Res., *56:* 1939–1947, 1996.
10. McDonough, W. S., Johansson, A., Joffee, H., Giese, A., and Berens, M. E. Gap junction intercellular communication in gliomas is inversely related to cell motility. Int. J. Dev. Neurosci., *17:* 601–611, 1999.
11. Koochekpour, S., Merzak, A., and Pilkington, G. J. Extracellular matrix proteins inhibit proliferation, upregulate migration, and induce morphological changes in human glioma cell lines. Eur. J. Cancer, *31A:* 375–380, 1995.
12. Novak, U., and Kaye, A. H. Brain tumor invasion: many cooks can spoil the broth. J. Clin. Neurosci., *6:* 455–463, 1999.
13. Lehmann, U., Gloeckner, S., Kleeberger, W., von Wasielevsky, H. F. R., and Kreipe, H. Detection of gene amplification in archival breast cancer specimens by laser-assisted microdissection and quantitative real-time polymerase chain reaction. Am. J. Pathol., *156:* 1855–1864, 2000.
14. McDonough, W., Tran, N., Giese, A., Norman, S. A., and Berens, M. E. Altered gene expression in human astrocytoma cells selected for migration: I. Thromboxane synthase. J. Neuropathol. Exp. Neurol., *57:* 449–455, 1998.
15. Ririe, K. M., Rasmussen, R. P., and Wittwer, C. T. Product differentiation by analysis of DNA melting curves during the polymerase chain reaction. Anal. Biochem., *245:* 154–160, 1997.
16. Roche Biochemicals LightCycler operator's manual, Version 3.0, 2000.
17. Rasmussen, R. P., Morrison, T., Herrmann, M., and Wittwer, C. T. Quantitative PCR by continuous fluorescence monitoring of a double-strand DNA specific binding dye. Biochemica, *2:* 8–11, 1998.
18. Morrison, T. B., Weis, J. J., and Wittwer, C. T. Quantification of low-copy transcripts by continuous SYBR Green I monitoring during amplification. Biotechniques, *24:* 954–958, 960, 962, 1998.
19. Vlodavsky, I., Levi, A., Lax, I., Fuks, Z., and Schlessinger, J. Induction of cell attachment and morphological differentiation in a pheochromocytoma cell line and embryonal sensory cells by extracellular matrix. Dev. Biol., *93:* 285–300, 1982.
20. Jones, P. A. Construction of an artificial blood vessel wall from cultured endothelial and smooth muscle cells. Proc. Natl. Acad. Sci. USA, *76:* 1882–1886, 1986.
21. Taylor, G. A., Hudson, E., Reseau, J., and Vande Woude, G. F. Regulation of P311 expression by met-hepatocyte growth factor/scatter factor and the ubiquitin/proteasome system. J. Biol. Chem., *275:* 4215–4219, 2000.
22. Bittner, M., Meltzer, P., Chen, Y., Jiang, Y., Seftor, E., Hendrix, M., Radmacher, M., Simon, R., Yakhini, Z., Ben-Dor, A., Sampas, N., Dougherty, E., Wang, E., Marincola, F., Gooden, C., Lueders, J., Glatfelter, A., Pollock, P., Carpten, J., Gillanders, E., Leja, D., Dietrich, K., Beaudry, C., Berens, M. E., Alberts, D., Sondak, V., Hayward, N., and Trent, J. M. Molecular classification of cutaneous malignant melanoma by gene expression profiling. Nature (Lond.), *406:* 536–540, 2000.
23. Page, B., Page, M., and Noel, C. A new fluorometric assay for cytotoxicity measurements *in vitro*. Int. J. Oncol., *3:* 476, 1993.
24. Studler, J. M., Glowinsky, J., and Levi-Strauss, M. An abundant mRNA of the embryonic brain persists at a high level in cerebellum, hippocampus, and olfactory bulb during adulthood. Eur. J. Neurosci., *5:* 614–623, 1993.
25. Giese, A., Rief, M. D., Loo, M. A., and Berens, M. E. Determinants of human astrocytoma migration. Cancer Res., *54:* 3897–3904, 1994.
26. Giese, A., Loo, M. A., Rief, M. D., Tran, N., and Berens, M. E. Substrate for astrocytoma invasion. Neurosurgery, *37:* 294–302, 1995.
27. Mariani, L., Beaudry, C., McDonough, W. S., Demuth, T., Hoelzinger, D. S., Ross, K. R., Berens, T., Coons, S. W., Watts, G., Trent, J. M., Wei, J. S., and Berens, M. E. Glioma cell motility is associated with reduced transcription of proapoptotic and proliferation genes: a cDNA microarray analysis. J. Neuro-oncol., in press, 2001.
28. Schiffer, D., Giordana, M. T., Mauro, A., and Migheli, A. Reactive astrocytes in the morphologic composition of peripheral areas of gliomas. Tumori, *74:* 411–420, 1988.
29. Zapata, E. J. Astrocytes in brain tumours. Differentiation or trapping? Histol. Histopathol., *9:* 325–332, 1994.
30. Lamszus, K., Laterra, J., Westphal, M., and Rosen, E. M. Scatter facto/hepatocyte growth facto (SF/HGF) content and function in human gliomas. Int. J. Dev. Neurosci., *17:* 517–530, 1999.
31. Stocker, M., Gherardi, E., Perryman, M., and Gray, J. Scatter factor is a fibroblast-derived modulator of epithelial cell mobility. Nature (Lond.), *327:* 239–242, 1987.
32. Gherardi, E., Gray, J., Stocker, M., Perryman, M., and Furlong, R. Purification of scatter factor, a fibroblast-derived basic protein that modulates epithelial interactions and movement. Proc. Natl. Acad. Sci. USA, *86:* 5844–5848, 1989.